Dynamic strength behavior of a Zr-based bulk metallic glass under shock loading*

Yu Yu-Ying(俞宇颖)†, Xi Feng(习 锋), Dai Cheng-Da(戴诚达), Cai Ling-Cang(蔡灵仓), Tan Ye(谭 叶), Li Xue-Mei(李雪梅), Wu Qiang(吴 强), and Tan Hua(谭 华)

Laboratory for Shock Wave and Detonation Physics Research, Institute of Fluid Physics, Chinese Academy of Engineering Physics, Mianyang 621900, *China*

(Received 25 November 2014; revised manuscript received 5 February 2015; published online 10 April 2015)

Dynamic strength behavior of $Zr_{51}Ti_5Ni_{10}Cu_{25}Al_9$ bulk metallic glass (BMG) up to 66 GPa was investigated in a series of plate impact shock-release and shock-reload experiments. Particle velocity profiles measured at the sample/LiF window interface were used to estimate the shear stress, shear modulus, and yield stress in shocked BMG. Beyond confirming the previously reported strain-softening of shear stress during the shock loading process for BMGs, it is also shown that the softened Zr-BMG still has a high shear modulus and can support large yield stress when released or reloaded from the shocked state, and both the shear modulus and the yield stress appear as strain-hardening behaviors. The work provides a much clearer picture of the strength behavior of BMGs under shock loading, which is useful to comprehensively understand the plastic deformation mechanisms of BMGs.

Keywords: shock loading, dynamic strength, bulk metallic glass

PACS: 62.20.de, 62.20.F–, 62.50.Ef, 64.70.pe **DOI:** 10.1088/1674-1056/24/6/066201

1. Introduction

Bulk metallic glasses (BMGs) are intriguing materials with unique properties, including high compressive strength, large elasticity, good corrosion resistance, etc.[1,2] The mechanical behaviors of BMGs have been a subject of interest for a long time, and recent advances have been reviewed by Schuh *et al.*[3] and Trexler *et al.*[4] Although extensive research has been done, some aspects of the mechanical behaviors of such materials, such as strength behavior and deformation mechanisms, are not yet clearly understood.

The study of BMGs' dynamic strength behavior, describing the ability to resist deviatoric stresses, is crucially important for understanding their deformation mechanisms, and for improving their structural performance under various loading conditions. Most early dynamic strength experiments on BMGs were conducted under uniaxial stress loading by using Kolsky bar techniques,[5,6] which were limited to relatively low stress around several gigapascals, and to intermediate strain rates around 10^3/s. Recently, shock wave methods, which provide access to a much higher pressure and strain rate than can be obtained in the aforementioned experiments, have been used to study the dynamic strength behavior of BMGs.[7–11] Yuan *et al.*[7] conducted pressure-shear impact experiments on $Zr_{41.25}Ti_{13.75}Ni_{10}Cu_{12.5}Be_{22.5}$ up to 8.8 GPa and found negligible effect of normal stress/hydrostatic pressure on the strength of this Zr-based BMG. Turneaure *et al.*[8,9] performed plane shock wave experiments on another Zr-based BMG, $Zr_{56.7}Cu_{15.3}Ni_{12.5}Nb_{5.0}Al_{10.0}Y_{0.5}$, up to 16.4 GPa. In contrast to the pressure-shear impact experiments, the phenomena of shear stress loss were observed in particle velocity profiles obtained from plane impact experiments, and were confirmed by simulating profiles with a strain-softening strength model. Recent work from Jaglinski *et al.*[10] showed that the strength of $(Hf_{0.5}Zr_{0.5})_{56.7}Cu_{15.3}Ni_{12.5}Nb_{5.0}Al_{10.0}Y_{0.5}$ up to 16 GPa behaves in a manner similar to its Hf-free BMG.[8,9] With free-surface velocity profiles, we obtained the shear stress on the Hugoniot state up to 27 GPa for $Zr_{51}Ti_5Ni_{10}Cu_{25}Al_9$ by comparing shock stress to hydrostatic pressure, and the strain-softening effect was also obvious.[11] The shear stress softening in BMG under shock compression was also found in the molecular dynamics (MD) simulation for a binary BMG ($Cu_{46}Zr_{54}$) performed by Arman *et al.*[12] As described above, the dynamic experiments on strength for BMGs are limited to low shock stress, and most are focused on the shock loading process. In fact, plate impact shock-release or shock-reload experiments are essential to comprehensively understand the dynamic strength behavior of various solid materials.[13–17]

In the current work, time-resolved plane impact experiments were performed on a Zr-based BMG ($Zr_{51}Ti_5Ni_{10}Cu_{25}Al_9$) up to 66 GPa to measure the shock-reload and shock-release particle velocity profiles. The self-consistent technique developed by Asay and Chabbildas[13] was used to analyze these profiles to estimate the comprehensive dynamic strength of this BMG, including the shear stress (τ_H) and shear modulus (G) on the Hugoniot state, and yield

*Project supported by the National Natural Science Foundation of China (Grant No. 11172281).

†Corresponding author. E-mail: yuyinyu@caep.cn

© 2015 Chinese Physical Society and IOP Publishing Ltd

stress (τ_c) when released or reloaded from the shocked state.

2. Experimental method

The samples used in this study are of the same composition ($Zr_{51}Ti_5Ni_{10}Cu_{25}Al_9$) as those used in our previous work[11,18] and were obtained from Liquid Metals Technology (Laboratory of the School of Materials Science and Engineering, Harbin Institute of Technology, China). The nominal density (ρ_0) for the samples used in this study is 6.740 g/cm^3 with a deviation of 0.004 g/cm^3 except for the sample used in shot No. 5, which is 6.655 g/cm^3. Ultrasonic sound velocities and elastic modulus for these samples at ambient conditions have been determined previously, and can be seen in Ref. [18]. The Zr-based BMG samples used in the shock loading experiments were plates with a nominal diameter of 26 mm and a thickness of about 3 mm. Both sides of the plates were finished parallel to an accuracy of 2 μm∼5 μm.

A modified reverse-impact technique[19] was adopted, and its configuration is schematically illustrated in Fig. 1. The impactor, viz., the Zr-based BMG sample, was backed with either a low-impedance material (polycarbonate), or a high-impedance material (stainless steel 304) to obtain the shock-release or shock-reload wave profiles, respectively. In contrast to the original reverse-impact method,[20] an 8-μm aluminum foil instead of a bulk Al-plate buffer was epoxy mounted on the LiF window. Such modification in the reverse-impact experiment enabled the distance interferometer system for any reflector (DISAR)[21] to record the particle velocity profile at the impact interface by excluding the effect of the transition wave in the bulk Al-plate buffer, which simplifies wave analysis. The impact velocity was measured by using a magnetically induced diagnostic system with an uncertainty of ∼0.5%. The dimensions of the impactor and window were considered to meet the uniaxial strain requirement during the experiment.

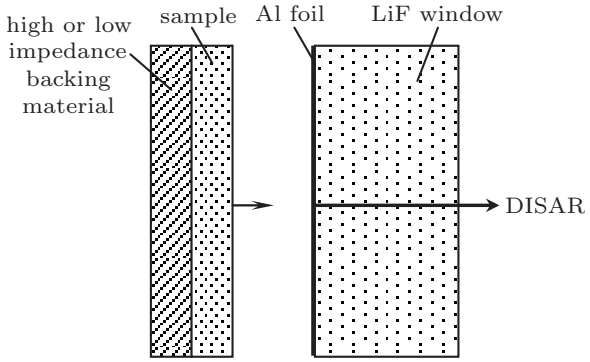


Fig. 1. Experimental configuration for the reverse plate-impact experiments.

3. Results and discussion

Three shock-release experiments and two shock-reload experiments were conducted on an ϕ32 mm bore two-stage light gas gun. The conditions of all of the five experiments are summarized in Table 1. All of the particle velocity profiles deduced from the recorded DISAR signals are shown in Fig. 2. Because of the split between the stainless steel 304 layer and the Zr-BMG impactor during launching, the higher pressure shock-reload experiment (shot No. 3) yielded an unexpected shock–release–reshock wave profile, and only the shock-release portion of this wave profile is used to estimate the strength behavior. The shock-reload experiment is the main hurdle to obtaining high pressure strength of solid materials, and new techniques need to be developed further.

Table 1. Experimental conditions and results for plate impact shock-release and shock-reload experiments.

Shot No.	Sample density ρ_0/(g/cm^3)	Sample thickness H_s/mm	Impactor velocity W/(km/s)	Shock stress σ_H/GPa	Shear modulus G/GPa	$(\tau_H+\tau_c)$/GPa	$(\tau_c-\tau_H)$/GPa
1[a]	6.744	3.142	2.889	37.28	47.59	1.73	–
2[b]	6.741	3.135	2.999	39.10	52.43	–	0.53
3[c]	6.743	3.120	3.604	49.69	63.25	1.88	–
4[a]	6.736	3.016	3.640	50.33	62.96	1.99	–
5[a]	6.655	3.007	4.480	66.42	79.47	2.39	–

[a] A polycarbonate buffer layer was used to support the Zr-BMG impactor (shock-release experiment).
[b] A stainless steel 304 buffer layer was used to support the Zr-BMG impactor (shock-reload experiment).
[c] Because of the split between the stainless steel 304 buffer layer and the Zr-BMG impactor during the acceleration process, this experiment yielded an unexpected shock–release–reshock wave profile, and only the shock-release wave profile was used to determine the $\tau_H+\tau_c$ by using Eq. (2a).

Using a centered, simple-wave analysis, the Lagrangian longitudinal wave speeds, C_L, during the release or reload process can be calculated from the particle velocity profiles by

$$C_L = \frac{h}{\Delta t - h/D}, \tag{1}$$

where h is the thickness of the Zr-BMG impactor, Δt is the time interval between the arrival of the release or reload wave at the window and the impact time, D is the shock wave velocity of the Zr-BMG sample which can be calculated by using an impedance matching technique with the Hugoniot data of Zr-BMG[18] and LiF.[22] Typical results of wave speeds during release and reload are illustrated in Fig. 3, in which *in situ* particle velocity u was corrected from the interface particle velocity by using the incremental impedance matching

technique,[23] u_H is the particle velocity in the shocked state, u_1 and u_2 are the particle velocities at the elastic–plastic transition point during the release and the reshock processes, respectively. The Lagrangian bulk wave speeds C_B during release and reload were evaluated by linearly extrapolating the lower plastic part of release.[13,19] A gradual transition from elastic wave to full plastic wave, referred to as quasielastic behavior,[24] is clearly presented for both release and reload processes.

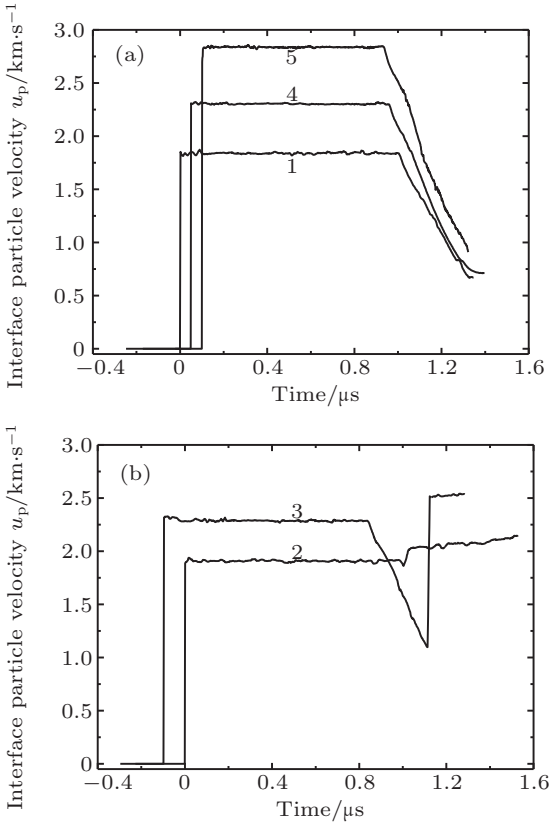


Fig. 2. Particle velocity profiles measured by DISAR at the impact interface for both shock-release experiments (a) and shock-reshock experiments (b). Time shift is adopted for clarity.

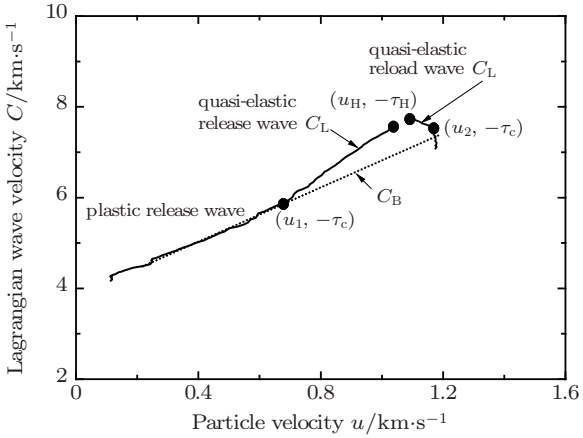


Fig. 3. Typical results of Lagrangian wave velocity (C_L and C_B) in Zr-based BMG as a function of the *in situ* particle velocity u.

Based on the extracted wave speeds, the shear stress in the shocked state, τ_H, and the yield stress, τ_c, defined at the yield point during the reload or release process were calculated by[13]

Release experiment:

$$\tau_c + \tau_H = -\frac{3}{4}\rho_0 \int_{u_H}^{u_1} \frac{C_L^2 - C_B^2}{C_L}\,\mathrm{d}u. \tag{2a}$$

Reload experiment:

$$\tau_c - \tau_H = \frac{3}{4}\rho_0 \int_{u_H}^{u_2} \frac{C_L^2 - C_B^2}{C_L}\,\mathrm{d}u, \tag{2b}$$

where ρ_0 is the initial density of the Zr-based BMG, u_H is particle velocity on the shocked state, u_1 and u_2 are velocities at the elastic–plastic transition point during the release and reload processes, respectively (as shown in Fig. 3). The shear modulus G on the shocked state was calculated through[25]

$$G = \frac{3}{4}\frac{\rho_0^2}{\rho}\left(C_L^2 - C_B^2\right), \tag{3}$$

where ρ is the shock compressed density of the Zr-based BMG.

The results of $\tau_H + \tau_c$, $\tau_c - \tau_H$ and G are also listed in Table 1. Based on the data of shots No. 1 and No. 2, the shear stress $\tau_H = 0.6$ GPa and the yield stress $\tau_c = 1.13$ GPa at a shock stress of 38 GPa (an average shock stress of shots No. 1 and No. 2) was determined. This implies that the Zr-based BMG supports only a small shear stress on the Hugoniot, but it can support a larger yield stress when released or reloaded from the Hugoniot state.

The data of shear stress τ_H, including previously reported data from our work[11] on the same BMG, are shown in Fig. 4(a). It is shown that the shear stress τ_H is nearly constant around 1.6 GPa in the shock stress range of 10 GPa–21 GPa, and then it drastically decreases to 0.6 GPa at 38 GPa. The decrease of shear stress τ_H with shock stress indicates the occurrence of a strain-softening effect, consistent with the experimental results,[8–11] and the MD simulation results from Arman *et al.*[12] (also shown in Fig. 4(a)). The variations of $\tau_H + \tau_c$ and G with shock stress σ_H are shown in Fig. 4(b) and Fig. 4(c), respectively. It is shown that both of them increase successively in the shock stress range of 37 GPa–66 GPa, implying the occurrence of a strain-hardening effect. This also means that this Zr-based BMG may be used as a structure material under high pressure up to 66 GPa. Considering the trend of the strain-softening of τ_H shown in Fig. 4(a), it is reasonable to suggest that the yield stress τ_c is the same strain-hardening property as $\tau_H + \tau_c$. Just for clarity, the yield stress τ_c in the shock stress range of 37 GPa–66 GPa was estimated by using the obtained data of $\tau_H + \tau_c$ with an assumption of a constant $\tau_H = 0.6$ GPa, and is also shown in Fig. 4(b). According to the above analysis, it can be seen that the Zr-based BMG exhibits complex strength behavior with the strain-softening effect during the shock loading process and the strain-hardening effect

during the release or reload process. Such complex strength behavior has also been reported in some ceramics by Vogler *et al.*[14,15]

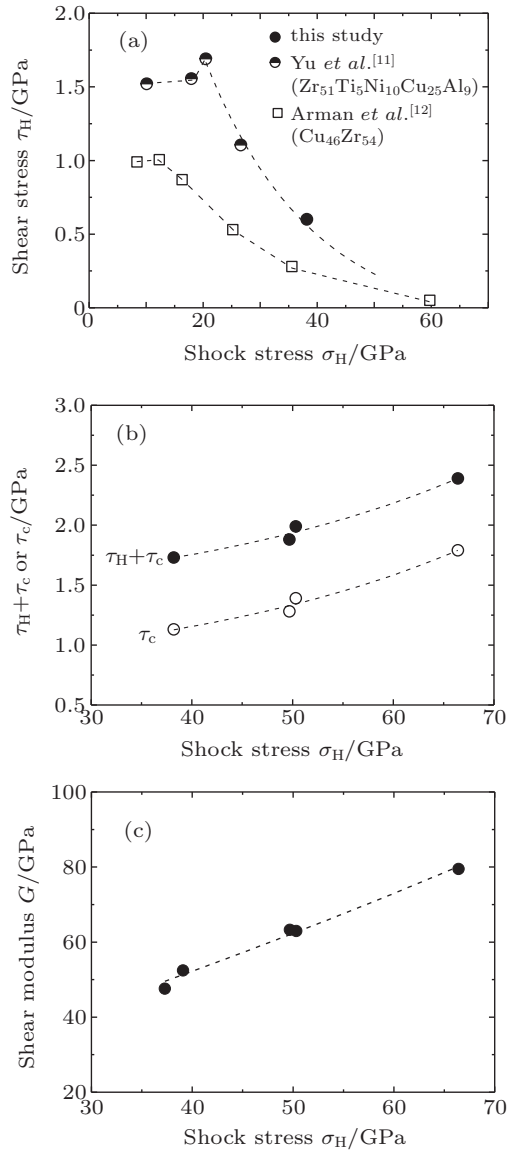


Fig. 4. Variations of the shear stress τ_H: (a), $\tau_H + \tau_c$, yield stress τ_c with an assumption of a constant $\tau_H = 0.6$ GPa (b) and shear modulus G (c) with shock stress σ_H. Dashed lines are just for clarity.

Commonly, shock-induced damage, failure and temperature are the main factors that cause the softening of the solid materials. However, with these factors, it is hard to explain the increase of the yield stress, and shear modulus with increasing shock stress. Arman *et al.*[12] suggested that the formation and evolution of shear transformation zones (STZs) during shock loading can decrease the fraction of structures with high shear resistance, and then cause the occurrence of strain softening in shear stress. Although their MD simulation results on the shear stress in the shocked state are similar to our present data, no data were present in Ref. [12] to confirm that such evolution of local structures in BMGs can cause a strain-hardening effect in the yield stress and shear modulus when released or reloaded from the shocked state. It is interesting to note the work from Shehadeh *et al.*[26] They also performed MD simulations on shock-induced plastic deformation, but in copper, and found that the shocked copper is rapidly relaxed from the uniaxial strain state to a near-hydrostatic state with small shear stress due to huge dislocation produced during ultrafast shock loading. Obviously, such a change in the stress state will notably reduce the shear stress in the Hugoniot state, but it will not damage the material or undermine the shear modulus and yield stress when released and reloaded from the Hugoniot state. Although the plastic deformation cell differs between metals and BMGs, it still could be suggested that the softening behavior of shear stress during the shock loading process, observed in BMGs, may be related to a possible change in stress state accompanied with the formation of localized shear bands under shock compression. In fact, the shear band is one of the explanations for the softening behavior of shear stress in shocked metals.[27] For hardening behavior of strength during release or reload from the shocked state, recent work by Zheng *et al.*[28] suggests that it can be ascribed to the interaction of the inclusions and shear bands in BMGs. Additional work is necessary to verify such a complex deformation mechanism in BMGs under shock loading.

4. Conclusion

In summary, plate impact shock-reload and shock-release experiments were performed on $Zr_{51}Ti_5Ni_{10}Cu_{25}Al_9$ up to 66 GPa to investigate the material's dynamic strength behavior. The variations of shear stress, yield stress, and shear modulus with shock stress for BMG are obtained by using the time-resolved particle velocity profiles, and they provide a much clearer picture of the strength behavior of Zr-BMGs under shock loading. Results show that the shock compressed Zr-based BMG supports only a small strength, but it retains high shear modulus and can support larger yield stress when released or reloaded from the Hugoniot state. Moreover, the strain-softening effect was observed during the shock loading process, while the strain-hardening effect was observed during release or reload from the shocked state.

Acnowledgments

K. C. Jin, W. Wang, M. L. Fang, Z. Y. Chen, and Y. M. Xiang are thanked for their experimental assistance.

References

[1] Johnson W L 1999 *MRS Bull.* **24** 42
[2] Inoue A 2001 *Amorphous and Nanocrystalline Materials: Preparation, Porperties and Applications* (Berlin: Springer) p. 1
[3] Schuh C A, Hufnagel T C and Ramamurty U 2007 *Acta Mater.* **55** 4067
[4] Trexler M M and Thadhani N N 2010 *Prog. Mater. Sci.* **55** 759
[5] Lu J and Ravichandran G 2003 *J. Mater. Res.* **18** 2039

[6] Lu J, Ravichandran G and Johnson W L 2003 *Acta Mater.* **51** 3429
[7] Yuan F P, Prakash V and Lewandowski J J 2010 *Mech. Mater.* **42** 248
[8] Turneaure S J, Winey J M and Gupta Y M 2006 *J. Appl. Phys.* **100** 063522
[9] Turneaure S J, Winey J M and Gupta Y M 2004 *Appl. Phys. Lett.* **84** 1692
[10] Jaglinski T, Turneaure S J and Gupta Y M 2012 *J. Appl. Phys.* **112** 063529
[11] Yu Y Y, Xi F, Dai C D, Cai L C, Tan H, Li X M and Hu C M 2012 *Acta Phys. Sin.* **61** 196202 (in Chinese)
[12] Arman B, Luo S, Germann T C and Çıağın T 2010 *Phys. Rev. B* **81** 14420
[13] Asay J R and Chhabildas L C 1981 *Shock Waves and High-Strain-Rate Phenomena in Metals* (New York: Plenum) p. 417
[14] Vogler T J, Reinhart W D and Chhabildas L C 2004 *J. Appl. Phys.* **95** 4173
[15] Vogler T J, Reinhart W D, Chhabildas L C and Dandekar D P 2006 *J. Appl. Phys.* **99** 023512
[16] Yuan F P, Tsai L, Prakash V, Dandekar D P and Rajendran A M 2008 *J. Appl. Phys.* **103** 103537
[17] Furnish M D, Alexander C S, Brown J L and Reinhart W D 2014 *J. Appl. Phys.* **115** 033511
[18] Xi F, Yu Y Y, Dai C D, Zhang Y and Cai L C 2010 *J. Appl. Phys.* **108** 083537
[19] Hu J B, Zhou X M and Tan H 2008 *Acta Phys. Sin.* **57** 2347 (in Chinese)
[20] Duffy T S and Ahrens T J 1995 *J. Geophys. Res.* **B100** 529
[21] Weng J D, Tan H, Wang X, Ma Y, Hu S L and Wang X S 2006 *Appl. Phys. Lett.* **89** 111101
[22] Marsh S P 1980 *LASL Shock Hugoniot Data* (Berkeley: University of California Press) p. 296
[23] Asay J R, Chhabildas L C and Dandekar D P 1980 *J. Appl. Phys.* **51** 4774
[24] Yu Y Y, Tan H, Hu J B, Dai C D, Chen D N and Wang H R 2008 *Acta Phys. Sin.* **57** 2352 (in Chinese)
[25] Yu Y Y, Tan H, Hu J B and Dai C D 2008 *Chin. Phys. B* **17** 264
[26] Shehadeh M A, Bringa E M, Zbib H M, McNaney J M and Remington B A 2006 *Appl. Phys. Lett.* **89** 171918
[27] Swegle J W and Grady D E 1986 *Metallurgical Applications of Shock-Wave and High-Strain-Rate Phenomena* (New York: Marcal Dekker) p. 705
[28] Zheng Q and Du J 2014 *J. Appl. Phys.* **115** 043519